

Steady-state stability of the generator – comparison of load angle calculated using *sine* and *cotangent* function, and new instability proximity index

Suad S. Halilčević** and Izudinka I. Kapetanović*

**University of Tuzla, Faculty of Electrical Engineering, Tuzla, 75000, Bosnia and Herzegovina ORCID: 0000-0002-6287-9300

*Bosnia and Herzegovina Telecom, Tuzla, 75000, Bosnia and Herzegovina

Corresponding Author: suad.halilcevic@unitz.ba

Submitted: 12-07-2021

Revised: 03-11-2021

Accepted: 02-12-2021

ABSTRACT

This paper presents two ways of calculating the load angle of a non-salient pole synchronous generator. The *sine* function used for calculation of the load angle of the generator considers its internal voltage, which with variable synchronous reactance introduces a double error in the calculation of the load angle. The *cotangent* function used for calculation of the generator's load angle is based on its active and reactive power and its external voltage. Another goal of this paper is to present the steady-state stability of the generator with a new instability proximity index based on the *cotangent* function of load angle calculation. A new instability proximity index is the energy porosity defined as an approximate measure of how far the current operating state of the generator is from the state of instability. The degree of danger of the generator entering an unstable state according to the relevant electrical quantities is especially emphasized by the sensitivity coefficients based on the new instability proximity index. The key findings from this research are found in the more accurate calculation of the load angle of the synchronous generator and in connection with that the accurate estimation of the distance of the generator from the point of instability. As the more accurate load angle is that calculated via the *cotangent* function and which is smaller than the load angle calculated via the *sine* function, it is possible to load the generator more with the same degree of stability compared to the load based on the load angle calculated via the *sine* function. This results not only in a better safety aspect of the generator operation, but also economically, because this approach in calculating the stability of the generator enables greater utilization of the generator capacity.

Keywords: Energy porosity; load angle; Steady-state stability.

INTRODUCTION

The question of stability of the electric power system is considered to have been fully addressed. There are many works on the issue, right from the 1920s (Steinmetz, 1920, Evans et al., 1924 & Wilkins, 1926), through the already famous works of (Crary, 1945 & Messerle et al., 1956) in the middle of the last century, till its end and the beginning of the twenty-first century (Kundur, 1994, Arjona et al., 1999, Savulescu et al., 1993, Kar et al., 1999, Kuo et al., 2002 & Sulistiawati, 2018). All these works treated the issue of power system stability as an issue of the whole system or as an issue of the system's components. Different approaches have been applied, such as those based on algebraic equations, such as the Routh-Hurwitz criterion (Parks, 1962), the Hermite stability criterion (Parks, 1977), and the Schur-Cohn criterion (Serban et al., 2007), then, linearized differential equations (Morgan, 2015), and those based on non-linear differential equations [Aeyels, 1998, Zhou et al., 2014 & Pyatnitskiy et al., 1996]. Further development was based on the state-space approach and methods of Lyapunov (Allaev, 2015). When artificial

intelligence techniques, such as neural networks, fuzzy logic, etc. emerged, many researchers applied these techniques to power system stability issues – especially to the voltage stability issues [Gao et al., 2019]. The researches were directed towards different aspects of system stability, such as steady-state, transient, frequency, rotor angle, and voltage stability (Kundur et al., 2004). However, the problem is multi-dimensional and multi-layered, with considerable overlaps among numerous aspects of stability. Power system stabilizers, power electronics, and contemporary microprocessor-based regulations offer secure and reliable solutions for power systems exposed to various disturbances. However, the problem of stability remains a challenge and offers opportunities for new views to arise and solutions to be offered.

This work considers one aspect of stability, steady-state stability, and investigates it in the context of one power system component, the synchronous generator. The steady-state stability of the synchronous generator (SSSG) takes into consideration the load angle, i.e., the angle between internal and external voltage vectors. The SSSG, and, with it, the change in load angle can be shown through a performance chart, a Cartesian diagram with reactive power Q and active power P on the x and y axis, respectively. The performance chart is constrained with practical steady-state stability in the under-excited generator area, then with the allowable temperature of the stator and rotor coils, and with the maximal and minimal values of power of turbine and field excitation current (Weedy et al., 2004). The generator operator uses the performance chart to tune the generator in such a way that P and Q of the generator stay in the internal area of the chart. For this, the operator needs an appropriate automatic regulation of voltage U and frequency f for which an automatic voltage regulator and automatic frequency regulator are used. For the first type of regulation, the generator must be equipped with a thyristor-based regulator of the system of excitation. For the second type of regulation, the generator's turbine (steam, hydro, or gas) must be equipped with a P - f regulator. This means that the generator's response to the changes in its operation is connected with complex acts; not with a single type of regulation, but with two.

It means that the load angle as a measure of SSSG is an angle-dependent on two factors: regulation of the field excitation current and regulation of frequency where one regulation follows the other and vice versa. Due to this, the load angle and SSSG cannot be viewed solely through the prism of active power (i.e., regulation of frequency), but through that of regulation of the field excitation current (i.e. regulation of terminal voltage) too. In other words, the induced electromotive force in the generator is a function of the magnetic flux change and the number of turns in the stator winding (armature). The connection of the resultant magnetic field of the generator with the electric power system is a function of the speed of the generator's rotor (magnetic flux change) and changes of field excitation current. Both phenomena are taken as apparent power, which comprises active power as a result of power force on the rotor shaft (change the rotor speed and, in accordance with it, the magnetic flux and electromotive force in the armature) and reactive power as a result of field excitation current change (change the electro-motive force behind synchronous reactance and, in accordance with it, the reactive power produced (or absorbed) by the generator, and change in the generator power factor too).

The magnitude of the internally generated voltage induced in a given stator is a function of numerous factors that include the construction of the machine, rotor flux, armature reaction flux, common generator flux, and rotation speed of the rotor.

The synchronous reactance of the machine is the sum of the armature leakage reactance and armature reaction reactance. The value of synchronous reactance depends on the distortion of the air gap magnetic field caused by the current flowing in the stator (armature reaction). A stator resistance R_a and X_s , add up to synchronous impedance Z_s , which is changed through the load changes on the generator, and because of that, the precise value of internal voltage cannot be calculated as the sum of measured output voltage and voltage drop in the stator coil (with constant Z_s). Another problem is that of the voltage applied across the field circuit, it is not mostly flat and constant over time but has a saw- tooth-like waveform.

The methods for the load angle determination by a procedure based on measured terminal voltage and rotor position signals are presented in (Barrera-Cardiel et al., 1999). In (Chen et al., 2000) the load angle is detected by the rotor position sensed with a photoelectric sensor mounted on the stator. The accuracy of these load angle estimation methods depends on the accuracy of the measurement of voltage and current, the possibility of mounting an encoder or sensor on the generator, and on parameters that determine the accuracy (equivalent resistance and reactance). In (Sumina et al., 2010) two methods for load angle determination on the salient-pole synchronous generator are presented. The first method is based on the measurement of rotor position (using an optical encoder) and power system

voltage. In the second method, the load angle estimation is based on the measured values of voltage and current of the synchronous generator. The accuracy of this load angle estimation method depends on the accuracy of voltage and current measurements and the quadrature-axis reactance X_q and resistance R .

In (Rahman et al., 2019), the monitoring of field quantities (voltage and current) and load angle measurement on the synchronous machine have been implemented successfully. These measurements are made in real-time, running all day every day, taking 60 samples per second. In (Wehbe et al., 2012) the least squares-based estimation of synchronous generator states and parameters with phasor measurement units (PMU) has been implemented to estimate the internal voltage of the generator. But, due to error in estimation and computational burden in these processes of calculation, the final estimate of the load angle could have serious errors and delays in it, which could lead to possible degradation of controls and analysis. In (Khanum et al., 2014 & Vilchis-Rodriguez et al., 2009) are presented the promising measurement hubs for real-time measurement of load angle and field excitation quantities. Estimation of load angles of synchronous machines using artificial neural networks and local PMU-based quantities has been presented in (Del Angel et al., 2007). As in each of the other measurement techniques, in this also there are problems with hardware and software solutions and their application. In the calculation of load angle, so far, there are two uncertain variables: synchronous reactance and, arising from it, the internal voltage of the generator. Finally, aspects of static stability in the presence of renewable energy sources are given in (Hou et al., 2020).

The main task of the power system is its stable operation, which is reflected in the appropriate load angle of the generators, frequency stability and voltage stability. Knowing the exact load angle of the generators enables the design of more stable and better controllers (Kien et al., 2021). The last works that can be found in the literature related to the calculation of the load angle is the work presented by (You, 2021), where a load angle measurement algorithm of synchronous generator adaptive to non-integer teeth ratio has been investigated. The algorithm proposed in this work uses the generator terminal voltage and the generator turbine teeth signal to calculate the generator load angle. In (Kumar&Babu, 2021) is presented a single machine to infinite bus power system by modelling it as Duffing equation with softening spring where through the method of multiple scales an approximate analytical expression which describes the variation of load angle is derived.

Many generators today operate with a load angle far below the limit value. The reason for this is the vigilance of the generator operator with regard to the actual value of the generator load angle, which cannot be determined with complete certainty by the above methods. The desire of the authors of this article is to determine which way of calculating the load angle gives the best results: the one over the function of the *sine* or *cotangent*. The first part of this paper presents a comparison of two ways of calculating the load angle: one is based on the *sinusoidal* function and the other on the *cotangent* function. The second part of this paper deals with the energy porosity of the generator in relation to its load angle and its steady-state stability. The paper ends with a conclusion and discussion.

METHODS FOR SOLVING THE PROBLEM OF CALCULATING THE LOAD ANGLE OF A SYNCHRONOUS GENERATOR

Through this section the load angle is shown via the *sine* and *cotangent* functions. Both cases were analyzed by the analytical-algebraic approach. The result of this analysis are the equations and their graphical representation. A new graphical representation of the load angle via the *cotangent* function can become a new more successful tool for power plant operators in generator control.

Load Angle of Synchronous Generator Calculated Using *Sine* Function

The SSSG is presented through the well-known relationship (with negligible stator winding resistance):

$$P = \frac{3U_f \cdot E}{X_s} \sin\delta \quad (1)$$

The load angle from 'Equation(1)' is given by:

$$\sin\delta = \frac{P \cdot X_s}{3U_f \cdot E} \Rightarrow \delta = \arcsin \left[\frac{P \cdot X_s}{3U_f \cdot E} \right] \quad (2)$$

Load Angle of Synchronous Generator Calculated Using *Cotangent* Function

On the other side, the load angle can be calculated as follows. The active power P of the generator is given as in 'Equation(1)' and the reactive power Q of the generator is given as in 'Equation(3)':

$$Q = -\frac{3U_f^2}{X_s} + \frac{3E \cdot U_f}{X_s} \cos \delta \quad (3)$$

The shunt capacities of the generator are ignored.

After several algebraic calculations, the formula for load angle calculation is obtained:

$$\begin{aligned} \cotan\delta &= \frac{\left(Q + \frac{3 \cdot U_f^2}{X_s} \right)}{P} \Rightarrow \\ \delta &= \operatorname{arccotan} \frac{\left(Q + \frac{3 \cdot U_f^2}{X_s} \right)}{P} = \operatorname{arccotan}(L), \text{ where} \\ L &= \frac{\left(Q + \frac{3 \cdot U_f^2}{X_s} \right)}{P} \end{aligned} \quad (4)$$

The load angle, Figure 1, describes the generator response to the load characterized by P and Q , without the need to measure or calculate the internal voltage E which cannot be precisely calculated due to changeable R and X_s .

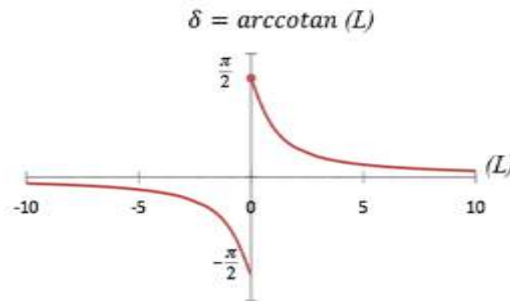


Figure 1. L - δ characteristic

The calculated load angle in 'Equation(4)' is the same as one presented in (Kundur, 1994), only that in (Kundur, 1994) the load angle is represented for generators with salient poles. The values for P and Q can be calculated from 'Equation(4)':

$$P = \frac{\left(Q + \frac{3 \cdot U_f^2}{X_s}\right)}{\cotan\delta} = \tan\delta \cdot \left(Q + \frac{3 \cdot U_f^2}{X_s}\right) \quad (5)$$

where changes in $P=f(\delta)$ are presented in Figure 2.

$$Q = P \cdot \cotan\delta - \frac{3 \cdot U_f^2}{X_s} \quad (6)$$

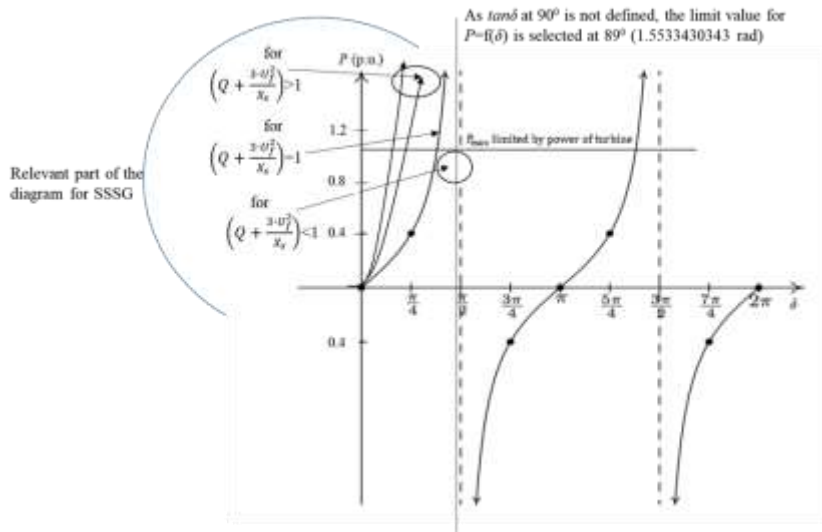


Figure 2. P as a function of δ (as $\tan\delta$ at 90° is not defined, the limit value for $P=f(\delta)$ is selected at 89°)

From 'Equation(5)' and 'Equation(6)' can be determined the extreme P and Q values:

$$P = 0 \text{ for } \cotan\delta = \infty (\delta = 0) \vee Q = -\frac{3 \cdot U_f^2}{X_s} \quad (7)$$

$$P = \infty \text{ for } \cotan\delta = 0 (\delta = \pi/2) \vee Q = \infty \quad (8)$$

$$Q = 0 \text{ for } P \cdot \cotan\delta = \frac{3 \cdot U_f^2}{X_s} \quad (9)$$

$$Q = \infty \text{ for } \cotan\delta = \infty (\delta = 0) \quad (10)$$

The reactive power is de facto constrained by I_{fmax} and active power is de facto constrained by the maximal power of the turbine. On the base of 'Equation(7)' to 'Equation(10)' and mentioned constraints, the operating chart for the generator can be formed as in Figure 3.

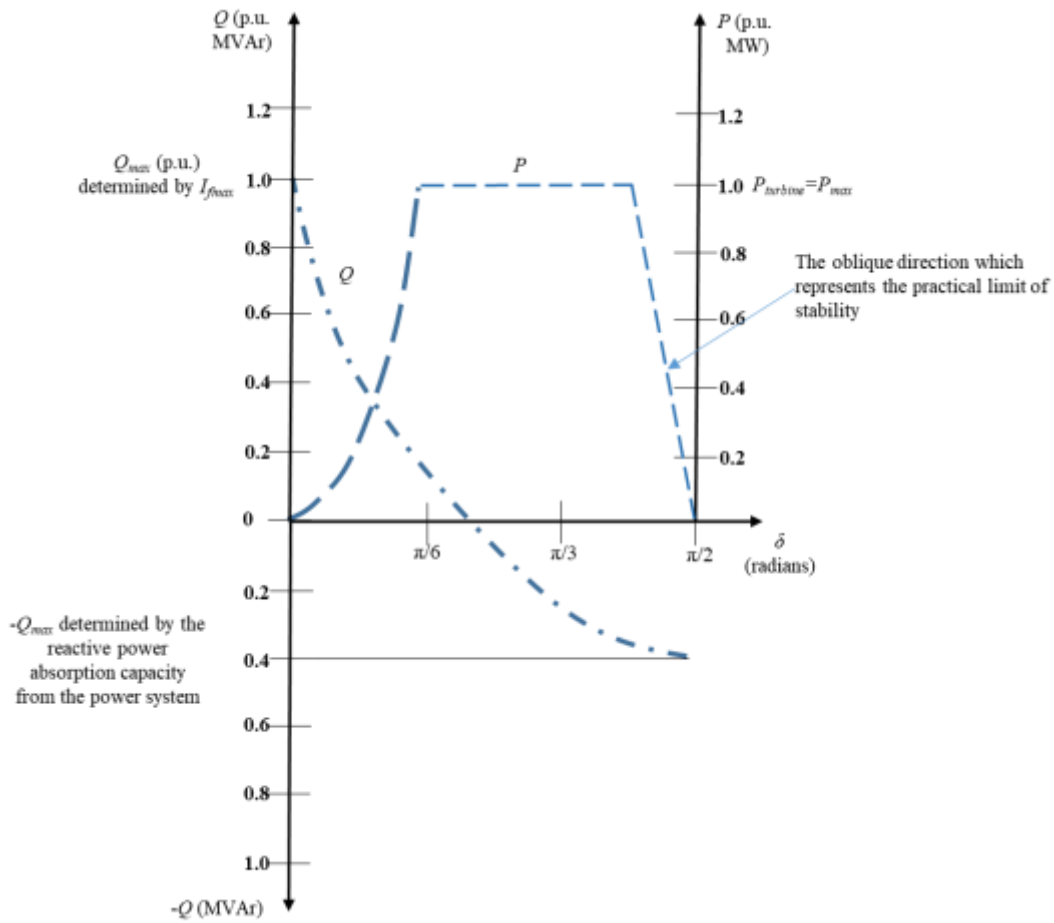


Figure 3. Operating chart of generator based on load angle calculation from 'Equation(7)' to 'Equation(10)'

Figure 4 shows two operating charts, one based on the classical operating chart of a generator (via $\sin\delta$) and the second based on the $\cot\delta$ presentation, by which are determined operating states of the generator for $\delta=30^\circ$.

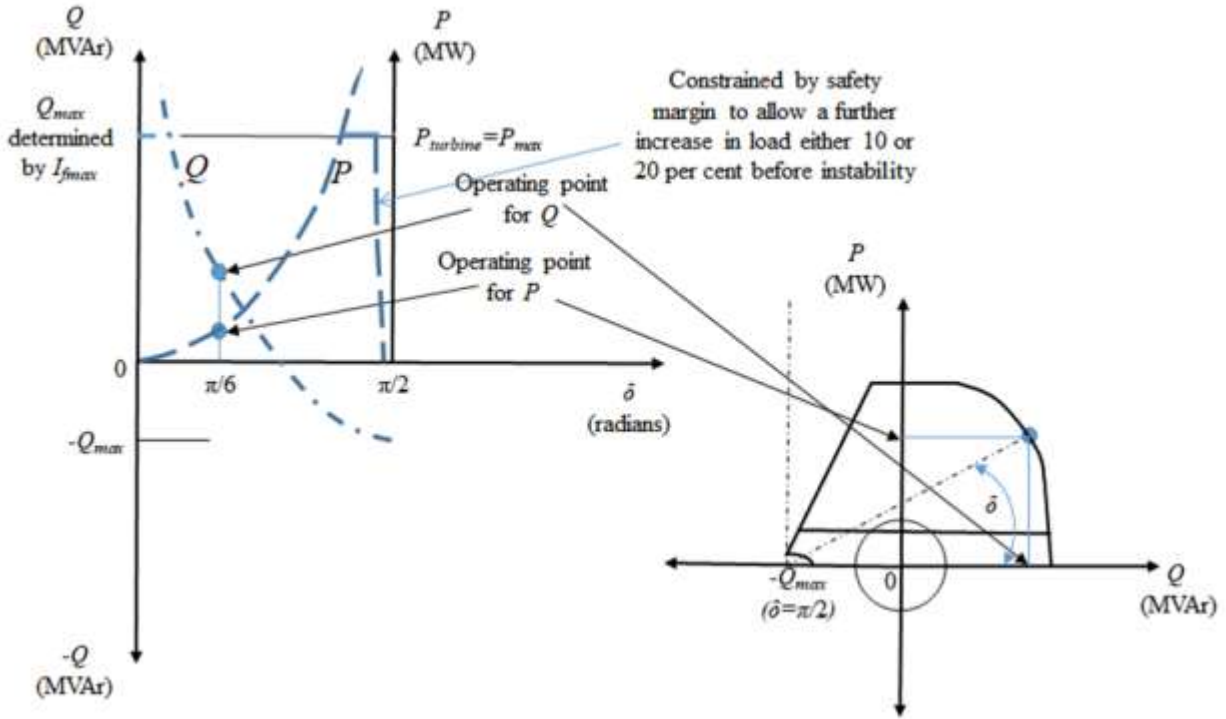


Figure 4. The operating point of the generator is presented in two ways; the load angle takes a value of 30°

Also, the presentation of P and Q changes on the $\cotan\delta$ platform for the inductive and capacitive regimes of the generator's operating state is presented in Figure 5.

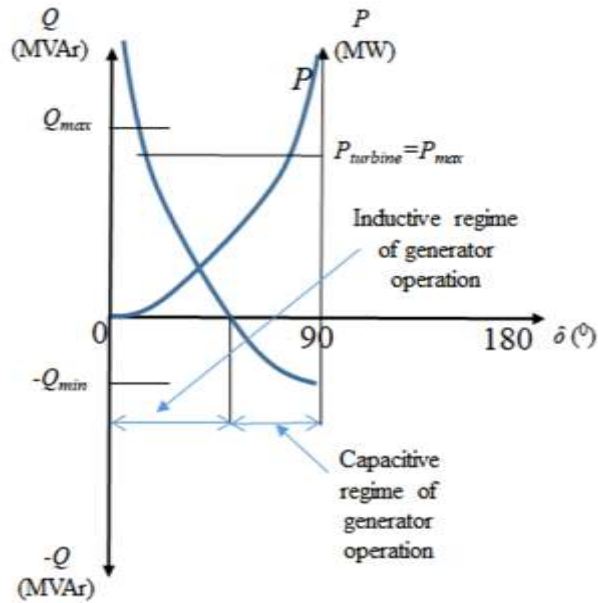


Figure 5. Inductive and capacitive regimes of generator operation

ENERGY POROSITY AS AN INDEX OF STEADY-STATE STABILITY OF SYNCHRONOUS GENERATOR

This analysis continues with the introduction of a dimensionless variable to assess the steady-state stability of the generator. This variable is called the energy porosity (*EPOR*) with respect to the load angle and the SSSG. The load angle obtained by 'Equation(4)' can be associated to the area through which mechanical and electrical energies "flow". It is the only space through which the generated mechanical and electrical energy interpenetrate and if this space is saturated, a stability problem arises.

Therefore, the energy porosity of the generator with respect to its load angle and its steady-state stability is defined as:

$$EPOR = \frac{|\cotan(90^\circ) - \cotan\delta|}{\cotan(89^\circ)} = \frac{|0 - \cotan\delta|}{0.017455} \approx 57.3 \cdot \cotan\delta = 57.3 \cdot \frac{\left(Q + \frac{3 \cdot U_f^2}{X_s}\right)}{P} = 57.3 \cdot L \quad (11)$$

The numerator in 'Equation(11)' represents a void space of the total load angle space represented by the denominator in 'Equation(11)'. As the $\cotan(90^\circ)$ is zero, to have a calculable *EPOR* and to be on the side caution when calculating *EPOR* and estimating the SSSG, the $\cotan(90^\circ)$ in the denominator of 'Equation(11)' is replaced by $\cotan(89^\circ) = 0.017455$. The relationship between *EPOR* and load angle is presented in Figure 6.

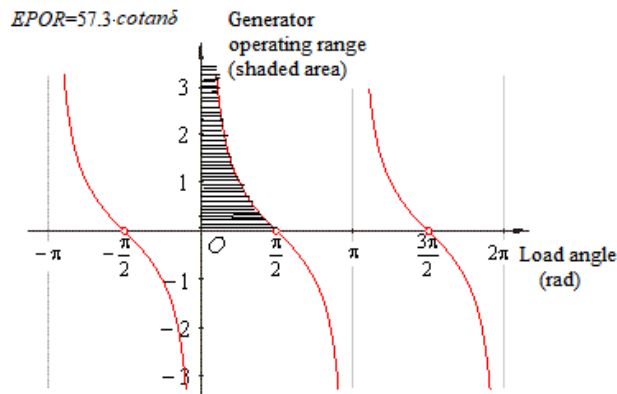


Figure 6. The relationship between *EPOR* and load angle (from $\cotan\delta$)

In the physical sense, theoretically, the porosity is infinite for unloaded generator (practically, it is limited by turbine power) and for point of the unstable operating state characterized by $\delta = \pi/2$, generator's porosity is characterized by the capacitive operating state with maximal reactive power engaged from the electric power network (leading working mode; absorb VAR in amount $-\frac{3U_f^2}{X_s}$).

MEASUREMENT AND CALCULATION RESULTS

Load Angle Calculation Using *Sine* and *Cotangent* Functions

To show the difference in the results of the calculation of SSSG using the functions of *sine* and *cotangent*, a synchronous generator with the following characteristics was selected: $U_n = 400$ V, $S = 10$ kVA, power factor lagging is

0.8, the synchronous reactance of $9 \Omega/\text{phase}$, and a neglected armature resistance. The phase voltage of this generator at rated condition could be calculated as follows:

$$U_f = \frac{400}{\sqrt{3}} = 231 \text{ V} \quad (12)$$

The armature current per phase at rated condition is:

$$I_A = \frac{S}{3 \cdot U_f} = \frac{10 \text{ kVA}}{3 \cdot 231} = 14,4 \text{ A} \quad (13)$$

The internally generated voltage at the rated condition is:

$$\begin{aligned} E &= U_f + R_A I_A + jX_s I_A = \\ &= 231 + 1,5 \cdot 14,4 + j(12 \cdot 14,4) = 306 \angle 30,2^\circ \text{ V} \end{aligned} \quad (14)$$

The active power P of the generator is:

$$P = 3 \cdot U_f \cdot I_A \cdot \cos \rho = 3 \cdot 231 \cdot 14,4 \cdot 0,8 = 8 \text{ kW} \quad (15)$$

and reactive power Q is:

$$Q = 3 \cdot U_f \cdot I_A \cdot \sin \rho = 3 \cdot 231 \cdot 14,4 \cdot 0,6 = 6 \text{ kVA} \quad (16)$$

The load angle calculated through $\sin \delta$ depends on of two uncertain variables (X_s and E) and the load angle calculated through $\cotan \delta$ depends on of one uncertain variable, X_s . From 'Equation(2)' and 'Equation(4)' can be calculated $\sin \delta$ and $\cotan \delta$, respectively, in amounts of 0.34 and 2.97. From these values, the load angles are $19,9^\circ$ and $18,6^\circ$.

Exact value of the load angle is obtained by measuring the duration of the pulse whose front edge is synchronized with the passage of the rotor through a certain position, and the rear edge with the passage of the fundamental harmonic voltage of one phase through zero. The obtained pulse duration time is proportional to the load angle. The rotor position detector is fixed and mounted on a fixed housing. An electrodynamic brake connected to a synchronous generator simulates different generator loads.

The hardware structure located in the Laboratory for Electrical Machines of the Faculty of Electrical Engineering, University of Tuzla, used for experiments is shown in Figure 7.



Figure 7. Hardware structure used to accurately measure load angle

The value of load angles for different operating states based on 'Equation(2)' and 'Equation(4)' can be seen in Table 1.

Table 1. Exact load angle (measured) and calculated using $\sin\delta$ and $\cot\delta$

S (kVA)	P (V)	Q (kW)	Q (kVAr)	Exact δ ($^\circ$)	$\sin\delta$ ($^\circ$)	$\cot\delta$ ($^\circ$)	Percentage error with respect to $\sin\delta$ (%)	Percentage error with respect to $\cot\delta$ (%)
10	106	.0	.0	19	.34 9.9	.97 8.6	5.2	2.1
8	88	.3	.8	15	.28 6.3	.58 5.6	3.2	1.3
6	73	.8	.6	12	.23 3.3	.45 2.7	3.1	1.6
5	66	.0	.0	10	.19 1.0	.72 0.9	1.8	0.92
8 or $\cos\phi=0.7$	89	.6	.7	13	.25 4.5	.2 3.4	11.5	3.0
Mean absolute percentage error (%)							4.9 6	1.78

The mean absolute percentage error of the load angle calculated using $\sin\delta$ in relation to the measured value, for a wide load range, is 4.96%. Moreover, the error in assessment of the load angle of the generator via the $\sin\delta$ function increases with decreasing $\cos\phi$ (power factor).

Energy Porosity Calculation

The values of *EPOR* for various input data are presented in Table 2.

Table 2. The *EPORs* and load angles for various operating states of generator

Case	S (kVA)	V	P (kW)	Q (kVAr)	$in\delta$ ($^{\circ}$)	$otan\delta$ ($^{\circ}$)	$EPOR$
	1010	06	.0	6	.34 0	.97 8.6	17 0*
	88	88	.3	.84	.28 6.3	.58 5.6	20 5
	673	73	.8	.63	.23 3.3	.45 2.7	25 5
	566	66	.0	.3	.19 1.0	.72 0.9	29 8**
	889 or $\cos\varphi=0.7$	89	.6	.75	.25 4.5	.2 3.4	24 0
	<p>* It means the worst level of SSSG among the presented operational states</p> <p>** It means the best level of SSSG among the presented operational states</p>						

The presentation of *EPOR* of generator operating state from the point of view of its steady-state stability enables us to research the aspects of that stability. The porosity of generator close to zero where $Q = -\frac{3U_f^2}{X_s}$ indicates the critical value of porosity and the need to bring the generator to an operating state of higher porosity.

The porosity of the synchronous generator from point of view of its steady-state stability is already depleted with *EPOR*=1, derived from 'Equation(11)', i.e., for $\cotan(89^\circ)=0.017455$. This arises from the need to calculate the *EPOR*, but in the physical sense of the word, *EPOR*=0 indicates the point of instability of the generator.

EPOR as a measure of SSSG and its proximity to an unstable operating state was analyzed in terms of its sensitivity to U_f , P , and Q changes. From 'Equation(11)' we obtain the following:

$$\frac{\partial EPOR}{\partial U_f} = \frac{343.8 \cdot U_f}{P \cdot X_s} \left(\frac{1}{V}\right) \quad (17)$$

$$\frac{\partial EPOR}{\partial P} = -57.3 \cdot \frac{QX_s + 3U_f^2}{P^2 \cdot X_s} \left(\frac{1}{kW}\right) \quad (18)$$

$$\frac{\partial EPOR}{\partial Q} = \frac{57.3}{P} \left(\frac{1}{kVAr}\right) \quad (19)$$

The *EPOR* increases, i.e., the load angle decreases with increased U_f , decreased P , and increased Q . For the given data ($P=8$ kW; $Q=6$ kVAr; $X_s=9$ ohm/phase; $\cotan\delta=2.97$; and $U_f=231$ V), the following *EPOR* sensitivity values were calculated with respect to U_f , P and Q :

$$\frac{\partial EPOR}{\partial U_f} = 1.1 \left(\frac{1}{V}\right); \quad \frac{\partial EPOR}{\partial P} = -20 \left(\frac{1}{kW}\right); \quad \frac{\partial EPOR}{\partial Q} = 7.16 \left(\frac{1}{kVAr}\right) \quad (20)$$

The results obtained indicate a much higher sensitivity of *EPOR* relative to P than to U_f and Q . Increasing of Q decreases the *EPOR* in the generator leading operating mode (in that case, Q is absorbed from the electric power system and has a negative sign).

CONCLUSION AND DISCUSSION

A comparison of the calculation of the load angle of a synchronous generator over two trigonometric functions is presented: $\cotan\delta$ and $\sin\delta$. It was found that the calculation of the generator load angle via the $\cotan\delta$ function is more accurate than the calculation that uses the \sin function of the load angle. The analysis shows that the calculation of the generator load angle via the \sin function leads to a lower level of the generator load compared to the case of the calculation of the load angle via the \cotangent function. Thus, the use of the \cotangent function to represent the load angle allows better utilization of the generator capacity under the same conditions of maintaining the stability of the generator. Using the \cotangent function avoids the need to know the internal voltage of the generator. It is advantageous for two reasons: first, the internal voltage is very difficult to measure, and second, due to the variable nature of synchronous reactance, the error of calculating the internal voltage of the generator based on this variable reactance propagates to the calculated value of the load angle. Calculation of the load angle via \cotangent requires three very available variables, P , Q , and the external voltage of the generator U_f . Furthermore, in this paper, SSSG is presented through the prism of energy porosity, a dimensionless measure of SSSG. The sensitivities of *EPOR* for the above mentioned three variables offer the complete view of the generator's operating state regarding its steady-state stability. These sensitivities make it possible to predict the effects of disturbances that may occur in the operation of the generator. Energy porosity is a new term and concept that enables the power plant operator to operate the generator more safely because it can predict exactly with defined sensitivity coefficients whether and how much change in the active and reactive power of the generator can lead to instability.

The accuracy of the proposed methodology was demonstrated on a test system simulated in a real environment, with measurements obtained from available hardware rather than through digital simulation. The

presented approach gives the best results of estimating the load angle of the generator in relation to those presented in the literature, it is the simplest and is not based on complex mathematical models that would require the engagement of computer hardware and software.

The next step on the way to the realization of the calculation of the load angle via the *cotangent* function is the calculation on the generator of higher power. Also, in this context, the economic benefit of calculating the load angle according to the *cotangent* function, and not according to the *sine* function, will be calculated.

The load angle expressed through the *cotangent* function will be applied to the problem of static stability of the multi-machine system using one of the approaches such as linearized state equations for system-level models or two-machines-infinite bus model system. In this sense, it will be interesting to see new values of the system stiffness (MW/Hz) and new eigenvalues and eigenvectors.

REFERENCES

- Aeyels, D., Peuteman, J., 1998.** A new asymptotic stability criterion for nonlinear time-variant differential equations. *IEEE Transactions on Automatic Control*, 43(7):968-971. doi: 10.1109/9.701102.
- Allaev, K.R., Mirzabaev, A.M., Makhmudov, T.F., Makhkamov, T.A., 2015.** Simplified Criterion of Steady-State Stability of Electric Power Systems. *Journal of Power and Energy Engineering*, 3:224-231. doi.org/10.4236/jpee.2015.34031.
- Arjona, M.A.L., Macdonald, D.C., 1999.** Saturation effects on the steady-state stability limit of turbine-generators. *IEEE Transactions on Energy Conversion*, 14(2):133-138.
- Barrera-Cardiel, E., Pastor-Gomez, N., 1999.** Microcontroller-based power-angle instrument for a power systems laboratory. In *Proceedings of the IEEE Power Engineering Society: Summer Meeting*. IEEE:1008-1012. doi: 10.1109/PESS.1999.787454.
- Chen, Y., Zhang, C., Hu, Z., Wang, X., 2000.** A new approach to real time measurement of power angles of generators at different locations for stability control. In *Proceedings of the IEEE Power Engineering Society: Winter Meeting*, 2:1237-1242.
- Crary, S.B., 1945.** *Power System Stability*. John Wiley and Sons, vol. I and II.
- Del Angel, A., Geurts, P., Ernst, D., Glavic, M., Wehenkel, L., 2007.** Estimation of rotor angles of synchronous machines using artificial neural networks and local PMU-based quantities. *Neurocomputing*, 70(16-18):2668-2678. doi.org/10.1016/j.neucom.2006.12.017.
- Evans, R.D., Bergvall, R.C., 1924.** Experimental analysis of stability and power limitations. *AIEE Trans.*, XLIII, 39-58.
- Gao, D.W., Wang, Q., Zhang, F., Yang, X., Huang, Z., Ma, S., Li, Q., Gong, X., Wang, F.Y., 2019.** Application of AI techniques in monitoring and operation of power systems. *Frontiers in Energy*, 13:71-85. doi.org/10.1007/s11708-018-0589-4.
- Hou, K., Li, Z., Chen, L., Xia, D., Li, Q., Xiao, Y., 2020.** Steady-State Stability of Sending-End System with Mixed Synchronous Generator and Power-Electronic-Interfaced Renewable Energy. *Mathematical Problems in Engineering*, ID 8693245. doi.org/10.1155/2020/8693245.
- Kar, N.C., Murata, T., Tamura, J., 1999.** Effects of Synchronous Machine Saturation, Circuit Parameters, and Control Systems on Steady State Stability. *Electric Machines and Power Systems*, 27(4):327-342. doi.org/10.1080/073135600268126.

Khanum, S., Ratnakar, K.L., Ramesh, K.N., Ravi, R., 2014. Evaluation of reactances and time constants of synchronous generator. *International Journal of Research in Engineering and Technology*, 03(special issue).

Kien, V.N., Trung, N.H., Quang, N.H., 2021. Design Low Order Robust Controller for the Generator's Rotor Angle Stabilization PSS System. *Emerging Science Journal*, 5(5):598-

618. doi: 10.28991/esj-2021-01299.

Kumar, M.G.S., Babu, C.A., 2021. Slow flow solutions and stability analysis of single machine to infinite bus power systems. *International Journal of Emerging Electric Power Systems*. 10.1515/ijeeps-2020-0176.

Kundur, P., 1994. *Power System Stability and Control*. McGraw-Hill.

Kundur, P., et al., 2004. Definition and classification of power system stability-IEEE/CIGRE joint task force on stability terms and definitions. *IEEE Transactions on Power Systems*, 19(3):1387-1401. doi: 10.1109/TPWRS.2004.825981.

Kuo, S.C., Wang, L., 2002. Steady-State Performance of a Self-Excited Induction Generator Feeding an Induction Motor. *Electric Power Components and Systems*, 30(6):581-593. doi.org/10.1080/15325000290084975.

Messerle, H.K., Bruck, R.W., 1956. Steady-state stability of synchronous generators as affected by regulators and governors. *Proceedings of the IEE - Part C: Monographs*, 103(3):24-34. doi: 10.1049/pi-c.1956.0003.

Morgan, R., 2015. *Linearization and Stability Analysis of Nonlinear Problems*. Rose-Hulman Undergraduate Mathematics Journal 16(2).

Parks, P.C., 1962. A New Proof of the Routh-Hurwitz Stability Criterion Using the Second Method of Lyapunov. *Proc. Cambridge Phil. Soc. Math. Phys. Sci.*, 58:694-702. doi.org/10.1017/S030500410004072X.

Parks, P.C., 1977. A new proof of Hermite's stability criterion and a generalization of Orlando's formula. *International Journal of Control*, 26(2):197-206. doi.org/10.1080/00207177708922303.

Pyatnitskiy, E.S., Rapoport, L.B., 1996. Criteria of asymptotic stability of differential inclusions and periodic motions of time-varying nonlinear control systems. *IEEE Transactions on Circuits and Systems I: Fundamental Theory and Applications*, 43(3):219-229. doi: 10.1109/81.486446.

Rahman, T., Sankaran, S., Seeley, N., Garg, K., 2019. Capturing Generator Rotor Angle and Field Quantities – SDG&E Experience and Approach to Using Non-traditional Generator Measurements. Presented at 69th Annual Conference for Protective Relay Engineers. Published in *Synchronous Generator Protection and Control: A Collection of Technical Papers Representing Modern Solutions*. doi.org/10.1109/CPRE.2016.7914880.

Savulescu, S.C., Oatts, M.L., Pruitt, J.G., Williamson, F., Adapa, R., 1993. Fast steady-state stability assessment for real-time and operations planning. *IEEE Transactions on Power Systems*, 8(4):1557-1569. doi: 10.1109/59.260960.

Serban, I., Najim, M., 2007. A new multidimensional Schur-Cohn type stability criterion. *American Control Conference*:5533 – 5538.

Steinmetz, C.P., 1920. Power control and stability of electric generating stations. *AIEE Trans.*, XXXIX(2), 1215-1287.

Sulistiwati, I.B., Soeprijanto, A., Wibowo, R.S., 2018. Determination of Generator Steady State Stability Limit for Multi-machine System based on Network Losses Concept. *The 3rd International Conference on Electrical Systems, Technology, and Information*. EDP Sciences.

Sumina, D., Šala, A., Malarić, R., 2010. Determination of Load Angle for Salient-pole Synchronous Machine. *Measurement Science Review*, 10(3):89-96. Symposium (NAPS), Champaign, IL. doi: 10.1109/NAPS.2012.6336346.

Vilchis-Rodriguez, D., Acha, E., 2009. A Synchronous Generator Internal Fault Model Based on the Voltage-Behind-Reactance Representation. *IEEE Transactions on Energy Conversion*, 24:184-194. doi: 10.1109/TEC.2008.2005281.

Weedy, B.M., Cory, B.J., 2004. *Electric Power Systems*. Wiley&Sons, England.

Wehbe, Y., Fan, L., Miao, Z., 2012. Least Squares Based Estimation of Synchronous Generator States and Parameters with Phasor Measurement Units. Presented at North American Power

Wilkins, R., 1926. Practical aspects of system stability. *AIEE Trans.*, 41-50.

You, J.H., 2021. A Load Angle Measurement Algorithm of Synchronous Generator Adaptive to Non-Integer Teeth Ratio. *The Journal of Korean Institute of Information Technology*, 19(8):75-89. doi: 10.14801/jkiit.2021.19.8.75.

Zhou, X.F., Hu, L.G., Jiang, W., 2014. Stability criterion for a class of nonlinear fractional differential systems. *Applied Mathematics Letters*, 28: 25-29. doi: 10.1016/j.aml.2013.09.007.